


# Testing for changes in biomass dynamics in large-scale forest datasets

Ervan Rutishauser<sup>1</sup>  | Stuart J. Wright<sup>1</sup> | Richard Condit<sup>2</sup> | Stephen P. Hubbell<sup>3</sup> | Stuart J. Davies<sup>4,5</sup> | Helene C. Muller-Landau<sup>1</sup>

<sup>1</sup>Smithsonian Tropical Research Institute, Ancon, Panama

<sup>2</sup>Morton Arboretum, Lisle, IL, USA

<sup>3</sup>Department of Ecology and Evolutionary Biology, University of California, Los Angeles, CA, USA

<sup>4</sup>Center for Tropical Forest Science-Forest Global Earth Observatory, Smithsonian Tropical Research Institute, Panama City, Panama

<sup>5</sup>Department of Botany, National Museum of Natural History, Washington, DC, USA

## Correspondence

Ervan Rutishauser, Smithsonian Tropical Research Institute, Box 0843-03092 Balboa, Ancon, Panama.  
Email: er.rutishauser@gmail.com

## Funding information

US Department of Energy; National Science Foundation; Smithsonian Tropical Research Institute; MacArthur Foundation

## Abstract

Tropical forest responses to climate and atmospheric change are critical to the future of the global carbon budget. Recent studies have reported increases in estimated above-ground biomass (EAGB) stocks, productivity, and mortality in old-growth tropical forests. These increases could reflect a shift in forest functioning due to global change and/or long-lasting recovery from past disturbance. We introduce a novel approach to disentangle the relative contributions of these mechanisms by decomposing changes in whole-plot biomass fluxes into contributions from changes in the distribution of gap-successional stages and changes in fluxes for a given stage. Using 30 years of forest dynamic data at Barro Colorado Island, Panama, we investigated temporal variation in EAGB fluxes as a function of initial EAGB ( $EAGB_i$ ) in  $10 \times 10$  m quadrats. Productivity and mortality fluxes both increased strongly with initial quadrat EAGB. The distribution of EAGB (and thus  $EAGB_i$ ) across quadrats hardly varied over 30 years (and seven censuses). EAGB fluxes as a function of  $EAGB_i$  varied largely and significantly among census intervals, with notably higher productivity in 1985–1990 associated with recovery from the 1982–1983 El Niño event. Variation in whole-plot fluxes among census intervals was explained overwhelmingly by variation in fluxes as a function of  $EAGB_i$ , with essentially no contribution from changes in  $EAGB_i$  distributions. The high observed temporal variation in productivity and mortality suggests that this forest is very sensitive to climate variability. There was no consistent long-term trend in productivity, mortality, or biomass in this forest over 30 years, although the temporal variability in productivity and mortality was so strong that it could well mask a substantial trend. Accurate prediction of future tropical forest carbon budgets will require accounting for disturbance-recovery dynamics and understanding temporal variability in productivity and mortality.

## KEYWORDS

biomass dynamic, carbon fluxes, long-term change, tropical forests

## 1 | INTRODUCTION

Understanding tropical forest responses to atmospheric and climate change is critical to modeling the future global carbon cycle. Repeated censuses of forest inventory plots have found increasing

stocks of tree carbon in apparently undisturbed tropical forests in Amazonia (Baker et al., 2004; Phillips et al., 1998), Africa (Lewis et al., 2013), and Borneo (Qie et al., 2017). Globally, analysis of long-term forest inventories suggests that old-growth tropical forests are currently carbon sinks, sequestering an average

of 0.34 Mg C ha<sup>-1</sup> year<sup>-1</sup> (confidence intervals [CIs] = 0.17–0.47; Muller-Landau, Detto, Chisholm, Hubbell, & Condit, 2014), albeit with a reduction in sink strength over time (Brienen et al., 2015; Qie et al., 2017). The causes of this increase and its consistency in space and time remain uncertain (Lewis, Lloyd, Sitch, Mitchard, & Laurance, 2009; Wright, 2010, 2013). Current knowledge of changes in old-growth tropical forest carbon stocks is hampered by limited spatial and temporal coverage of monitoring plots, sensitivity to measurement errors and data correction procedures, and the confounding influences of disturbance-recovery dynamics (Clark, Clark, et al., 2017; Muller-Landau et al., 2014).

There are multiple pathways through which anthropogenic global change could increase or decrease carbon stocks and fluxes in old-growth tropical forests. Increasing atmospheric carbon dioxide could enhance tropical tree growth and forest productivity through increased photosynthesis and water use efficiency (Lloyd & Farquhar, 2008), and thereby increase forest carbon stocks (Figure 1a–c). Alternatively, rising temperatures and increasing drought frequency and/or intensity could increase tree mortality and thereby decrease forest carbon stocks (McDowell et al., 2018). The “Bigger and Faster” hypothesis proposes that growth, recruitment, and mortality are all increasing (Clark, Clark, et al., 2017); in this case, the net effect on biomass depends on the relative magnitude of the increases in productivity and mortality (Figure 1d–f). Some but not all studies have found evidence of increasing productivity (Brienen et al., 2015; Feeley, Wright, Supardi, Kassim, & Davies, 2007; Körner, 2015) and increasing mortality (Brando et al., 2014; Brienen et al., 2015; Liu et al., 2017; McDowell et al., 2018; Phillips et al., 2010).

It is also possible that the observed increase in tropical forest biomass is due not to global change influences but to long-lasting recovery from past disturbances in some (but not all) tropical forests (Figure 1g–i; Wright, 2010). There is growing evidence that past human-induced or climatic disturbances continue to profoundly shape current forest composition (Brncic, Willis, Harris, & Washington, 2006; Levis et al., 2017; Magnabosco Marra et al., 2018), functioning (Doughty et al., 2015; McMichael, Matthews-Bird, Farfan-Rios, & Feeley, 2017; Oslisly et al., 2013), and extent (Mayle, Burbridge, & Killeen, 2000) in tropical regions. Forest succession after disturbance would generate a pattern of increasing total biomass mortality and biomass productivity over time, similar to that expected under the “Bigger and Faster” hypothesis (Clark, Clark, et al., 2017), and constitutes a null hypothesis or non-global change hypothesis. Forest recovery post-disturbance poses a particular challenge, as it may act at various spatial and temporal scales, and in only a subset of tropical forests.

We propose to separate out the contributions of disturbance-recovery dynamics to temporal variation in forest carbon stocks by decomposing changes in whole-plot biomass fluxes into contributions from changes in the distribution of gap-successional stages and changes in fluxes for a given stage (Figure 2). An old-growth tropical forest is a shifting mosaic of patches at different stages of recovery (Watt, 1947; Whitmore, 1989), of which most are increasing in biomass at any given time (Körner, 2003a). Dividing a plot into small quadrats provides a simple operational way to characterize this mosaic of

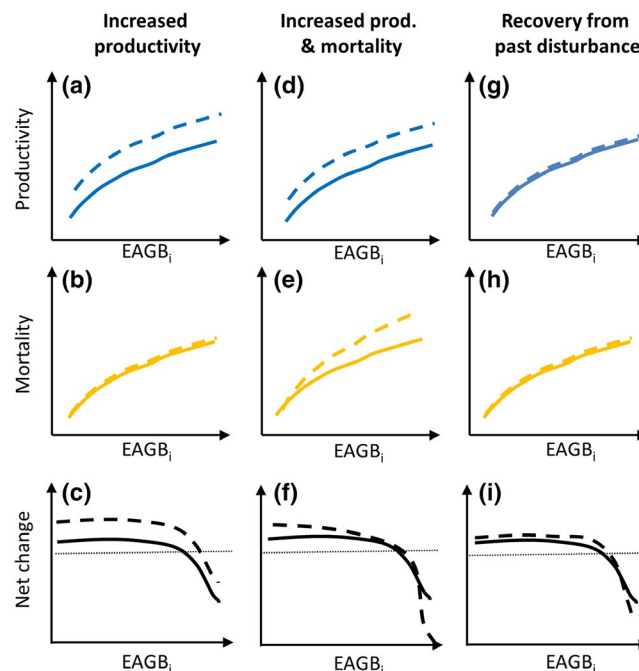


**FIGURE 1** Expected patterns of quadrat biomass fluxes in relation to initial estimated above-ground biomass ( $EAGB_i$ ) for three possible scenarios (columns) consistent with increasing biomass stocks in tropical forests. In every panel, the solid line shows the pattern expected for an earlier census interval, and the dashed line for a later census interval. Increasing productivity due to “fertilization” (first column), means higher productivity for a given  $EAGB_i$  in the second census interval (a, dashed line) than in the first one (a, solid line), no systematic difference in mortality after controlling for  $EAGB_i$  (b), and thus higher net change in  $EAGB_i$  per  $EAGB_i$  in the second census interval (c). Increasing productivity and mortality, as expected under “speeding up” (second column), means higher productivity and higher mortality in the second census interval (d, e) and diverse possible patterns for net change (f). Finally, recovery from disturbance (final column) is expected to show no systematic change in fluxes when controlling for  $EAGB_i$  (g–i). Note that local quadrat productivity increases with initial quadrat  $EAGB_i$  in all scenarios and census intervals (first row, blue), as does the local mortality flux (second row, yellow). Quadrat-level biomass net change (third row, black) is the difference between productivity and mortality fluxes, and is positive for low  $EAGB_i$ , and becomes negative for high  $EAGB_i$ .

stages, and quadrat initial  $EAGB_i$  ( $EAGB_i$ ) provides a useful proxy for age/time since disturbance (Bormann & Likens, 1979; Denslow, Ellison, & Sanford, 1998). Plot-level  $EAGB_i$  fluxes (Figure 2c) then reflect the integration of functions for fluxes as a function of  $EAGB_i$  (Figure 2a) with the distribution of  $EAGB_i$  (Figure 2b). Both quadrat productivity and mortality fluxes (Mg/ha) are expected to increase with  $EAGB_i$  (Figure 2a), and consistent global change influences should be evident in directional changes in these functions over time—that is, in increases or decreases in fluxes when controlling for  $EAGB_i$ . Climate variation could also contribute to temporal variation in productivity and mortality drivers, and thus in fluxes for a given  $EAGB_i$  (Dong et al., 2012). In contrast, the distribution of quadrat  $EAGB_i$  depends largely on the disturbance history at a site (Espírito-Santo et al., 2014; Fisher, Hurtt,

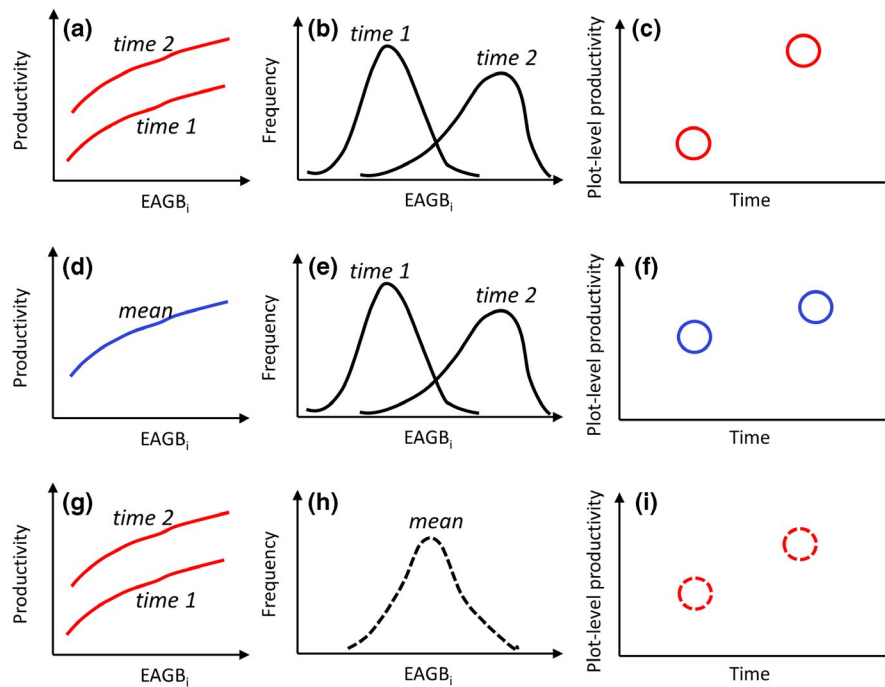


**FIGURE 2** Whole plot estimated above-ground biomass (EAGB) fluxes (right column) in a given time period depends on the combination of how small-scale fluxes vary with initial EAGB ( $EAGB_i$ ) (left column) and how  $EAGB_i$  varies spatially across the plot and over time (middle column). Here, we illustrate this for productivity; the same integration holds for whole-plot mortality. To distinguish the contribution of flux- $EAGB_i$  relationships from the contribution of  $EAGB_i$  distributions to plot-level biomass dynamics, we estimated what whole-plot fluxes would be in each census interval if either the flux- $EAGB_i$  relationship or the  $EAGB_i$  distribution were constant across census intervals. To calculate a single constant flux- $EAGB_i$  relationship (d) and a single constant  $EAGB_i$  distribution (h), we averaged across all census intervals weighted equally. We then integrated the empirical flux- $EAGB_i$  relationship over the  $EAGB_i$  distribution for each census interval under three scenarios: (i) interval-specific flux- $EAGB_i$  relationships and interval-specific  $EAGB_i$  distributions (a-c); (ii) the average flux- $EAGB_i$  relationship and interval-specific  $EAGB_i$  distributions (d-f); (iii) interval-specific flux- $EAGB_i$  relationships and the average  $EAGB_i$  distribution (g-i)

Thomas, & Chambers, 2008), and can fluctuate from a dominance of early successional (i.e., low  $EAGB_i$ ) stages soon after disturbance (Figure 2b, time 1) to higher frequency of late successional quadrats longer after disturbance (Figure 2b, time 2).

Using a large-scale, long-term forest plot dataset for Barro Colorado Island (BCI), Panama, we seek to disentangle the influences of disturbance recovery from potential global change by quantifying how local biomass dynamics vary with initial biomass, and evaluating whether these relationships change over time. Specifically, we tested for temporal variation in quadrat productivity, loss, and net change in biomass when controlling for initial biomass. To assess the degree to which similar biomass patches were consistently associated with similar forest structure across census intervals, we also examined how quadrat initial biomass was related to tree density (per area) and mean tree size at each census and compared these relationships over time.

## 2 | METHODS

### 2.1 | Study site

Barro Colorado Island is located in central Panama (9°08' N, 79°51'0" W). Temperature averages 27°C and annual rainfall averages 2,657 mm (for 1926–2017; Paton, 2018), with a dry season between January and April. The vegetation is moist tropical

forest. The 50 ha forest dynamics plot was established in 1982 (Condit, 1998; Hubbell et al., 1999), and recensused in 1985 and every 5 years subsequently (Figure S1). All free-standing woody stems with a diameter at breast height (DBH)  $\geq 1$  cm were mapped, tagged, and identified to species, and were measured in diameter at every census in which they remained alive. Diameter measurements were taken at 1.3 m height or above any buttress or major stem deformity. We omitted the initial census of 1982–1983 from analyses of biomass and biomass dynamics due to major differences in the field measurement methods for large trees (Condit, 1998), leaving seven censuses and six 5 year intervals between 1985 and 2015. We omitted 1.2 ha of swamp and 1.9 ha of young forest from the analysis due to differences in species composition, structure, and dynamics (Condit, Hubbell, & Foster, 1996; Harms, Condit, Hubbell, & Foster, 2001), leaving 46.9 ha for analysis. (We note, however, that our results are robust to the inclusion of the young forest, as we would expect; see Supporting information C1). Supplemental materials provide additional details on the census methods (Supporting information A).

### 2.2 | Individual tree biomass calculation

For all stems of dicot (non-palm) species, we estimated above-ground biomass (EAGB) from individual DBH and species-specific

wood density (WD) using a generic tropical forest biomass equation (Chave et al., 2014). For stems measured at heights other than 1.3 m, we first calculated taper-corrected equivalent diameters at 1.3 m height using a generic taper correction equation for BCI:

$$DBH = D \times \exp(0.0247 \times (HOM - 1.3)),$$

where  $D$  is diameter measured at height of measurement (HOM; in m; equation 2, Cushman, Muller-Landau, Condit, & Hubbell, 2014). We applied this taper correction to avoid time-dependent biases in plot-level biomass stocks and fluxes associated with changes over time in the proportion of trees measured above 1.3 m and average measurement heights (Cushman et al., 2014). We also estimated missing diameter measurements (1,192 of the 2,607,014 records) by simple linear interpolation between consecutive measurements. We then EAGB (in Mg dry biomass) of each stem in each census from its DBH, using the updated version of equation 7 of Chave et al. (2014), incorporating species-level WD (in g/cm<sup>3</sup>) collected near the study site (Wright et al., 2010 and unpublished) and a climatic index that represents environmental influences on tree height allometries ( $E = 0.05645985$  for BCI):

$$EAGB = \exp(-2.024 - 0.896 \times E + 0.920 \times \log(WD) + 2.795 \times \log(DBH) - 0.0461 \times \log(DBH)^2)$$

(see Supporting information S2 for details of wood density assignment).

For palms, we estimated biomass using a palm-specific allometric equation based on DBH. For palm species that do not grow in DBH (all local palm species except *Socratea exorrhiza*), we first assigned species-specific median DBH to each palm stem in each census (Table S1). We EAGB (in Mg dry biomass) of each palm stem as

$$AGB = 0.0417565 \times DBH^{2.7483},$$

based on the family-wise specific allometric equation of Goodman et al. (2013), modified to include the log-transformation correction factor (Baskerville, 1972). We recognize that this procedure results in systematic errors in biomass fluxes for palms that do not grow in diameter, because it fails to consider their height growth, and that better estimates would be possible if height data were available. Overall, palms other than *Socratea* account for 0.9% of the woody biomass and 1.8% of the estimated woody productivity on BCI.

For multi-stemmed trees, individual tree biomass was calculated as the sum of biomass of all live stems. Large (DBH > 50 cm) individuals of strangler fig species (*Ficus costaricana*, *Ficus obtusifolia*, *Ficus popenoei*, and *Ficus trigonata*), for which diameter measurements are unreliable measures of size, were excluded from the analysis by excluding associated quadrats (Table S2).

## 2.3 | Quadrat-level biomass stocks and fluxes

Biomass stocks and fluxes were analyzed at the scale of 10 m quadrats and for the plot as a whole. Analysis at the quadrat level aimed to quantify how local biomass fluxes vary with local initial biomass

for each census interval, and to compare these relationships across census intervals. Initial biomass was calculated as the sum of biomass of all trees alive at the initial census. We calculated biomass fluxes per time in productivity, mortality, and net change using simple arithmetic estimators. That is, we calculated fluxes for each quadrat by summing over relevant trees ( $i$ ) and dividing by the time interval measured separately for each tree:

$$EAGB \text{ change} = \sum \frac{(EAGB_{\text{final } i} - EAGB_{\text{initial } i})}{\text{time}_i}.$$

Productivity was calculated as the sum of the EAGB changes of surviving trees and the EAGB of recruits (including resprouts). Because the census dataset includes all stems >1 cm in diameter, biomass increment accounts for the vast majority of the woody productivity (97.5%; Figure S2). Biomass loss was calculated as the sum of EAGB<sub>*i*</sub> of all trees that died by the next census, as well as of large individual stems that died on multi-stemmed individuals (see Supporting information A for details on the treatment of multi-stemmed trees). For recruits and dead stems, the time interval used was the mean time between measurements for that quadrat and census interval. These arithmetic estimators systematically underestimate fluxes because they miss contributions from trees that recruited and died during the census interval, with larger biases for longer census intervals (Kohyama, Kohyama, & Sheil, 2019). However, all our census intervals were very similar in length (Figure S1), and thus, these biases do not confound our analysis. Estimated biomass stocks and fluxes are expressed on a quadrat basis (100 m<sup>2</sup>), and can be converted to units of Mg/ha by multiplying by 100.

We quantified the relationship of quadrat-level biomass fluxes to initial biomass for each census interval using local regression and power function fits. We first illustrate the relationships for productivity, mortality, and net change using local polynomial regression, specifically the *locfit()* function in R (Loader, 1999) with smoothing parameter (alpha) set to 0.7. To formally test for variation in EAGB productivity and loss among census intervals, each of these fluxes was modeled as power functions of EAGB<sub>*i*</sub>, with a power variance function structure (using package lme4; Bates, Mächler, Bolker, & Walker, 2015). We tested for differences among census intervals in power function “slopes” (exponents) and normalized intercepts, with these intercepts calculated as the predictions for the median EAGB value of 125.0 Mg/ha. CIs were computed by bootstrapping over quadrats (1,000 times). We evaluated the sensitivity of the results to different local regression models, and the consistency between the power function and local regression results.

For each census interval, our analyses of quadrat-level fluxes excluded quadrats affected by any one or more of three problems. First, analyses excluded quadrats if any stem had a change in HOM >10 cm during that census interval. Second, analyses excluded quadrats that ever had a strangler fig larger than 50 cm DBH. Finally, analyses excluded quadrats where an individual stem had an unreasonably large change in DBH in that census interval, such that its absolute biomass change was >0.98 Mg/ha (this threshold was

chosen because it is 20% of the mean productivity per hectare computed over all quadrats and census intervals that met the first two criteria). We excluded between 389 and 1,288 of the 4,669 possible quadrats (i.e., not in swamps or in young forest), depending on the census interval, mostly because of the first rule removing quadrats with a change in measurement height (Table S2). We did not remove or correct unlikely but less influential diameter changes, because in a dataset of this size, these random errors will tend to cancel out, whereas attempts to filter or correct such changes have strong potential to introduce systematic biases (because it is easier to detect some types of errors than others, Muller-Landau et al., 2014). The results were robust to varying filtering methods (Figure S7).

We evaluated consistency in or differences among censuses in the probability distribution of quadrat-level EAGB using empirical cumulative density functions. We specifically tested for differences among censuses in selected percentiles (5th, 10th, 25th, 50th, 75th, 90th, and 95th), by evaluating whether CIs overlapped. We estimated CIs on the percentiles by bootstrapping over quadrats.

We evaluated the sensitivity of our results to the spatial grain of quadrats, applying the same methods for smaller (8.33 m) and larger (12.5, 15.15 m) quadrats (Figures S8–S10).

## 2.4 | Disentangling sources of temporal variation in whole-plot fluxes

To distinguish the contribution of flux–EAGB<sub>i</sub> relationships from the contribution of EAGB<sub>i</sub> distributions to plot-level biomass dynamics, we estimated what whole-plot fluxes would be in each census interval if either the flux–EAGB<sub>i</sub> relationship or the EAGB<sub>i</sub> distribution was constant across census intervals. To calculate a single constant flux–EAGB<sub>i</sub> relationship and a single constant EAGB<sub>i</sub> distribution, we averaged across all census intervals weighted equally. We then integrated the empirical flux–EAGB<sub>i</sub> relationship over the EAGB<sub>i</sub> distribution (Figure 2) for each census interval under three scenarios: (a) interval-specific flux–EAGB<sub>i</sub> relationships and the average EAGB<sub>i</sub> distribution; (b) the average flux–EAGB<sub>i</sub> relationship and interval-specific EAGB<sub>i</sub> distributions; and (c) interval-specific flux–EAGB<sub>i</sub> relationships and interval-specific EAGB<sub>i</sub> distributions. For each flux–EAGB<sub>i</sub> relationship, fluxes for the central 90% of the EAGB<sub>i</sub> distribution (from the 5th to 95th percentile) were estimated from EAGB<sub>i</sub> using fits of the *locfit* function to the full distribution, as above ( $\alpha = 0.7$ ). In the tails of the distribution, fluxes were estimated as equal to the means for the corresponding interval (i.e., the 0–5th percentile interval or the 95th–100th percentile interval), to avoid undue influence of a few points.

## 2.5 | Forest structure

For each census interval, forest structure was quantified by analyzing the distributions over  $10 \times 10$  m quadrats of the numbers of trees  $\geq 1$ , 10, and 60 cm, and of quadratic mean diameter ( $D_g = \sqrt{\sum DBH^2/n}$ , in cm). We quantified how these structure measures varied with quadrat EAGB in each census interval by fitting local regressions (R

function *locfit* with  $\alpha = 0.7$ ), and calculating values expected for selected quadrat EAGB (corresponding to the 10th, 25th, 50th, 75th, and 90th percentiles computed for all censuses combined). We tested whether there were changes over time in the values expected for selected quadrat EAGB or in the plot-level means, by comparing CIs obtained by bootstrapping over quadrats.

## 3 | RESULTS

### 3.1 | Quadrat-level biomass fluxes

Mean quadrat EAGB productivity and EAGB mortality loss both increased with initial quadrat EAGB in each census interval, with uncertainty rising in parallel (Figures 3 and 4a,b; Figure S2). Both fluxes were well-fit by power functions of EAGB<sub>i</sub> (Figure 4a,b; Figures S5 and S6). Mean EAGB net change was positive for low EAGB<sub>i</sub> and became negative in quadrats with EAGB<sub>i</sub> > ~3 Mg/100 m<sup>2</sup> (equivalently 300 Mg/ha; Figure 4c).

There was substantial variation among census intervals in EAGB fluxes as a function of EAGB<sub>i</sub>. This is visually evident from examination of the differences in EAGB-specific fluxes from the mean flux over census intervals (Figure 4d–f), and is quantified by differences in parameter values of the power function fits (Figure 5; power functions were good fits to the data, as is evident from their concordance with local regressions in Figures S5 and S6). Productivity fluxes in the 1985–1990 census interval averaged 10%–30% higher than the mean over census intervals for all but the highest values of EAGB<sub>i</sub> (Figure 4d, blue line). The next highest productivity fluxes were in the most recent census interval, and the lowest productivity fluxes were in 2000–2005 (Table S6). EAGB loss also varied among census intervals, with above-average EAGB loss for lower EAGB<sub>i</sub> in some census intervals (2005–2010 and 2010–2015) and for higher EAGB<sub>i</sub> in other intervals (1995–2000). The power function fits reflected these patterns, with significant variation among census intervals in the normalized intercepts, the estimated fluxes at the midpoint of the EAGB<sub>i</sub> distribution (here 125 Mg/ha; Figure 5a,b; Table S6). For productivity, the first census interval had by far the largest intercept, with subsequent declines to 2000–2005, and then increases since 2005 (Figure 5a). For mortality, the intercept tended to increase after the 1990–1995 census interval. The slopes (exponents) of the power functions showed little variation among census intervals (mostly overlapping CIs, Figure 5c,d). CIs for EAGB loss and net flux were wide (Figures S3 and S4), limiting the power to test for significant differences among census intervals (Figure 4d–f; Figure S3 and S4). Results were qualitatively consistent for other quadrat sizes (Figures S8–S10).

### 3.2 | Whole plot biomass stocks and fluxes

The probability distribution of EAGB density over  $10 \times 10$  m quadrats varied only slightly among censuses, and showed no clear directional change (Figure 6a). The 5th–50th percentiles of quadrat EAGB increased slightly from 1985 to 2000, and then decreased again to values similar to initial ones (Figure 6c). In contrast, the 90th percentile increased slightly over the study period (Figure 6c).



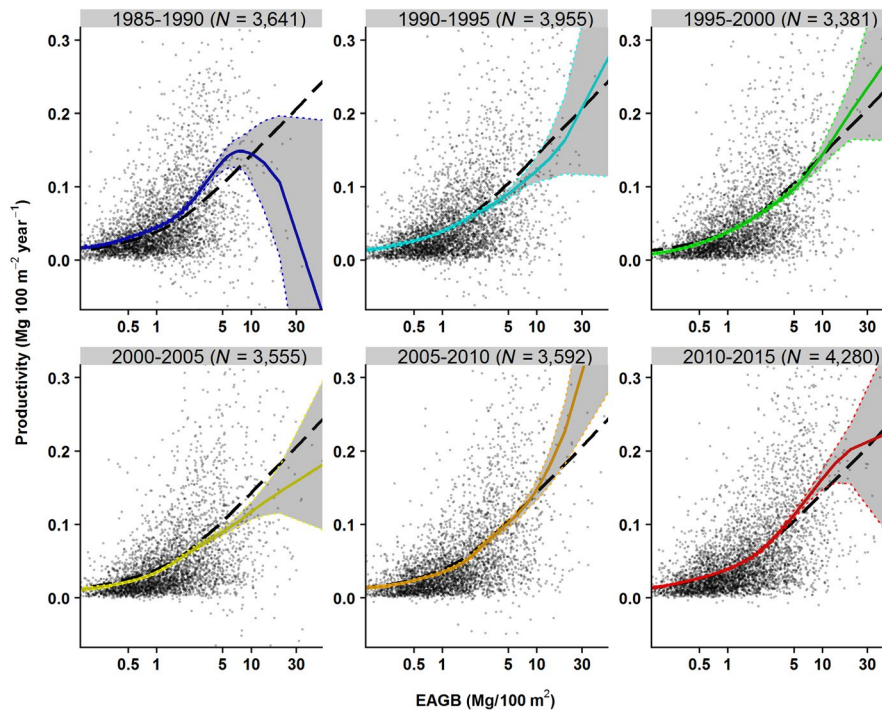


**FIGURE 3** Quadrat-level mean annual estimated above-ground biomass (EAGB) productivity ( $\text{Mg } 100 \text{ m}^{-2} \text{ year}^{-1}$ ) as a function of initial quadrat biomass (EAGB in  $\text{Mg}/100 \text{ m}^2$ ) for each 5 year census interval, for individual  $10 \times 10 \text{ m}$  quadrats (points), together with local polynomial regression lines for individual census intervals (colored solid lines) and for all census intervals combined (black dashed lines). Confidence envelopes were computed from bootstrapping over quadrats. For each census interval, analyses excluded quadrats with problematic EAGB change measurements (see Section 2 for details);  $N$  is the number of quadrats included for each census interval. The range of data shown here is truncated, but all points were included in the analyses. Note that EAGB stocks and fluxes can be converted to units of  $\text{Mg}/\text{ha}$  by multiplying by 100

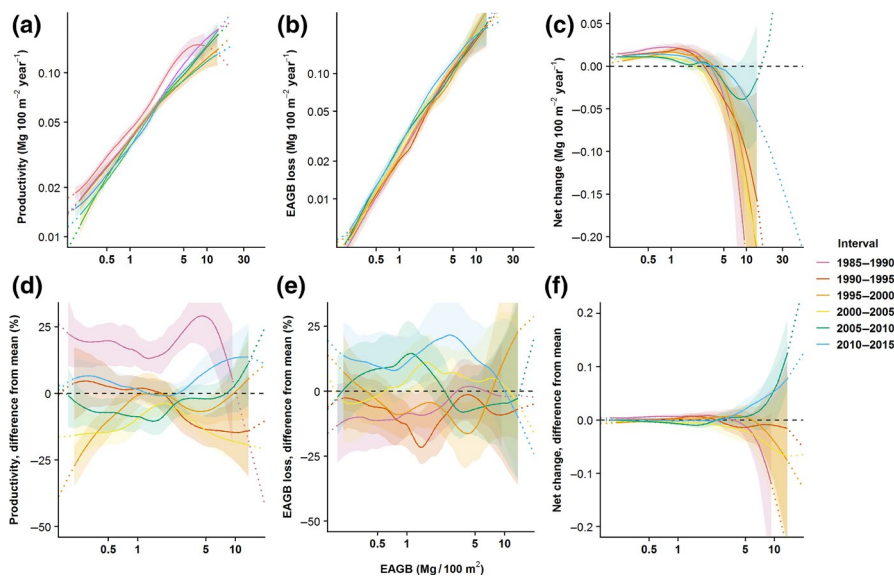


**FIGURE 4** Variation among census intervals in quadrat estimated above-ground biomass (EAGB) productivity (a), loss (b), and net change (c) as a function of above-ground biomass (EAGB) at the initial census for  $10 \times 10 \text{ m}$  quadrats, together with the corresponding differences from the mean (per initial EAGB) across all census intervals (d-f). Patterns were quantified using local polynomial regression; regression lines are displayed as solid lines for initial EAGB values spanning the 2nd–98th percentiles of the respective census interval, and as dotted lines outside this range. Confidence envelopes were computed by bootstrapping over quadrats, and are shown for the 2nd–98th percentiles of initial EAGB using shading. Analyses excluded quadrats with problematic EAGB change measurements (see methods for details). Note that productivity (a) and loss (b) are shown on log scales, and their differences from the mean are expressed in percentages (d,e) whereas the net change (c) and its difference from the mean (f) are shown on linear scales. Note that EAGB stocks and fluxes can be converted to units of  $\text{Mg}/\text{ha}$  by multiplying by 100

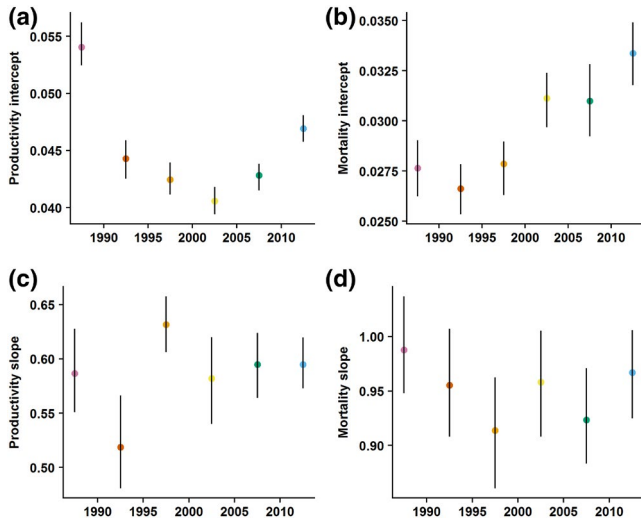


**FIGURE 5** Variation among census intervals in the intercepts (a, b) and slopes (c, d) of power function relationships of quadrat-level productivity (a, c) and losses to mortality (b, d) to initial above-ground biomass. Intercepts are normalized, and represent the values at the overall midpoint estimated above-ground biomass (EAGB) value ( $1.25 \text{ Mg}/100 \text{ m}^2$ , i.e., an EAGB density of  $125 \text{ Mg}/\text{ha}$ ). Confidence intervals were computed from bootstrapping over quadrats (see Table S2 for parameter values). Analyses excluded quadrats with problematic EAGB change measurements (see Section 2 for details)

Temporal variation in whole-plot EAGB fluxes as estimated by integrating temporal variation in flux-EAGB<sub>i</sub> relationships and EAGB<sub>i</sub> distributions was due almost entirely to temporal variation in flux-EAGB<sub>i</sub> relationships for a given EAGB<sub>i</sub>, with almost no contribution of temporal variation in the EAGB<sub>i</sub> distribution (Figure 7; Table S4 scenario b). Temporal patterns in whole-plot fluxes thus roughly mirrored those in fluxes as a function of EAGB<sub>i</sub>. Productivity flux was highest in 1985–1990, then dropped steeply, and has increased over the last three census intervals. Mortality loss flux dropped between the first and second census interval, and tended to increase since then, albeit CIs are wide. These patterns in estimated whole-plot fluxes mirrored calculated fluxes from summing over quadrats, although the exact pattern in productivity is highly sensitive to data cleaning and correction procedures (Figures S7–S17).

### 3.3 | Changes in forest structure

The mean density of stems  $>1 \text{ cm dbh}$  increased modestly after the 1982–1983 drought, then thinned rapidly from 1990 to 2005, and was stable from 2005 to 2015 (Figure 8a, black points and lines). The same pattern was evident when controlling for focal quadrat biomass density (Figure 8a, colored lines). The density of stems  $\geq 10 \text{ cm dbh}$  in the plot as a whole increased slowly to 1995 and then decreased to 2010, with parallel patterns in all but the lowest biomass quadrats (Figure 8b). The density of large stems ( $\geq 60 \text{ cm dbh}$ ) remained essentially constant over time (Figure 8c; Table S5). Quadratic mean

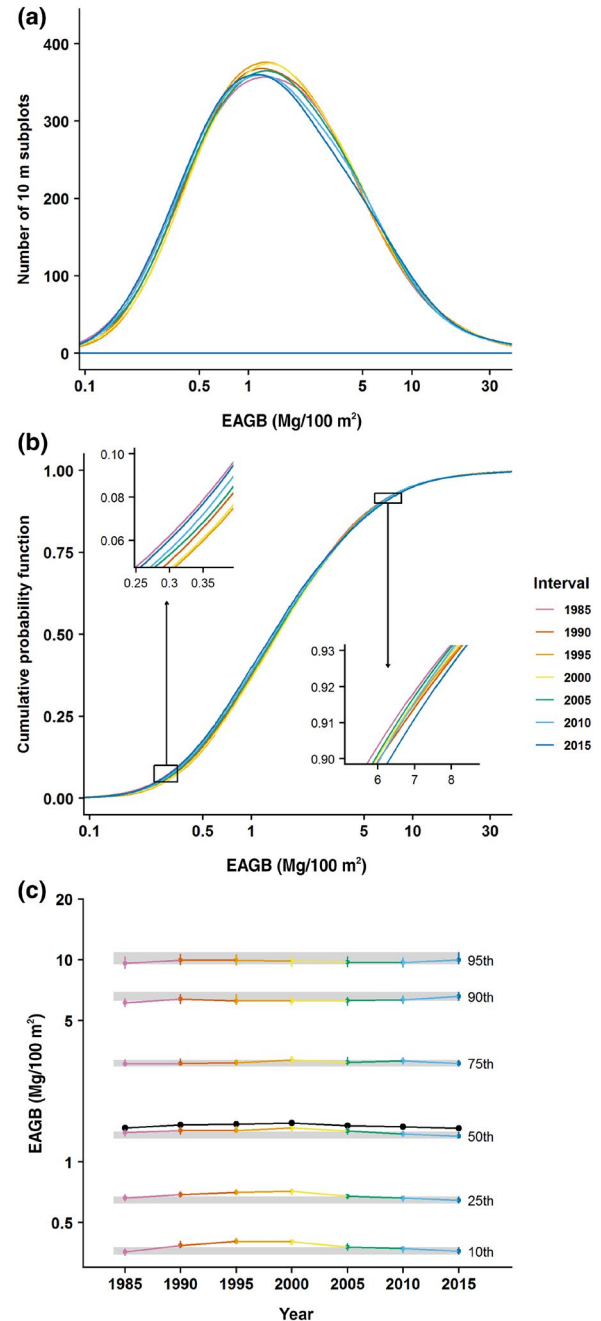


**FIGURE 6** Probability density distribution (a) and cumulative probability distribution (b) of estimated above-ground biomass (EAGB) density across all  $10 \times 10 \text{ m}$  quadrats, with insets in (b) magnified to show inter-census variation for cumulative probabilities of 0.05–0.1 and 0.9–0.95. (c) Variation over time in seven specific percentiles of the EAGB distribution over quadrats (colored points and lines) and in the overall mean EAGB density at the 50 ha scale (black solid points and lines). In panel (c), vertical lines show the 95% confidence intervals (CIs) from bootstrapping over quadrats, and horizontal gray shading shows the CIs for values in 2015 to enable easy visual assessment of how other years compare. The illustrated curves in panels (a) and (b) are truncated at the 0.2th and 99.8th percentiles of the distribution, but all values were included in analyses. Note that the EAGB densities can be converted to units of  $\text{Mg}/\text{ha}$  by multiplying by 100

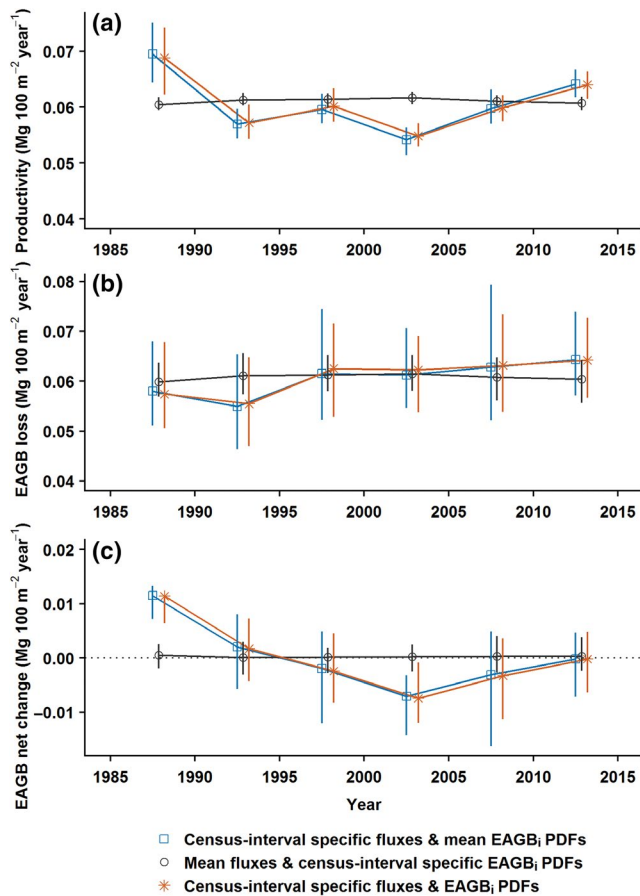


**FIGURE 7** Time series of hypothetical whole-plot productivity (a), loss (b), and net change (c) expected with and without variation among census intervals in functions specifying how estimated above-ground biomass (EAGB) fluxes vary with initial biomass, and with and without variation among census intervals in initial EAGB distributions ( $EAGB_i$ ). See Section 2 for details. Vertical lines show 95% confidence intervals obtained by bootstrapping over quadrats. The points are placed at the mid-points of the census intervals, and jittered horizontally to increase readability. Values are given in Table S3. Note that EAGB stocks and fluxes can be converted to units of Mg/ha by multiplying by 100. PDF, probability density function

stem DBH increased from 1985 to 2000, and then leveled off, with parallel patterns for all quadrat biomass densities (Figure 8d).

## 4 | DISCUSSION

Here, we proposed and applied a straightforward way to control for successional stage in analyses of forest biomass change, by comparing forest patches at similar stages of gap recovery, as inferred by similar  $EAGB_i$  density. Our analyses revealed strong temporal variation in forest woody productivity and loss fluxes both at the whole plot level and when controlling for local ( $10 \times 10$  m) gap phase. There was no consistent long-term trend in productivity, mortality, or biomass in this forest over 30 years, although the interannual variability in productivity and mortality is so strong that it could well mask a substantial trend. Woody productivity varied ~25% among 5 year

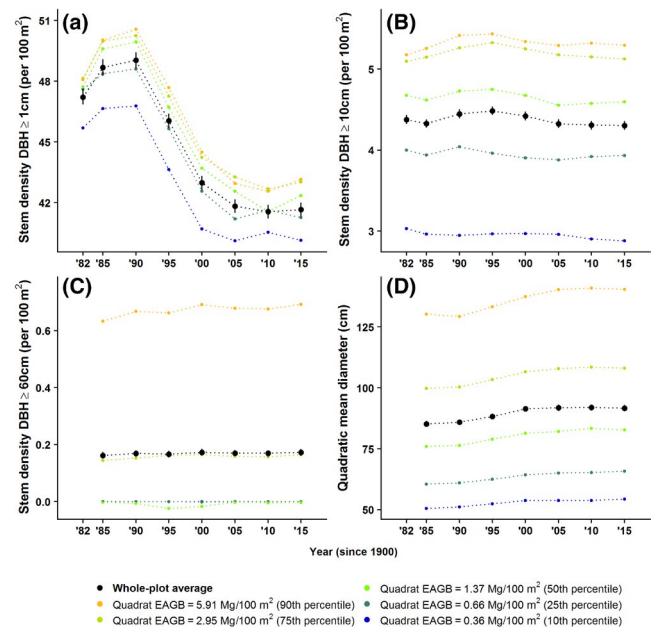


**FIGURE 8** Variation among censuses in forest size structure at the whole plot level (black) and for different initial EAGB in  $10 \times 10$  m quadrats (colors). 95% Confidence intervals (vertical lines) were obtained from bootstrapping over quadrats, but are generally smaller than the dot size. The density of large stems and mean diameter are not reported for 1982 due to inconsistencies in measurement methods (Condit, 1998). DBH, diameter at breast height

census intervals, and woody losses ~15%, between 1985 and 2015. Because this variability is consistent even after controlling for gap phase, we conclude it arises from interannual variation in driving factors, most obviously climate.

### 4.1 | Temporal climate variation in the tropics and its impacts

Tropical forests experience biologically important interannual climate variation in temperature, solar radiation, water availability, and the frequency and intensity of major storms. Interannual climate variation in tropical forests is related in part to irregularly periodic climate oscillations, including the El Niño Southern Oscillation (ENSO) and the Atlantic Multidecadal Oscillation (AMO). In much of the tropics, the El Niño phase of ENSO is associated with drier, sunnier, and hotter conditions, whereas the La Niña phase is associated with wetter, cloudier, and cooler conditions (Holmgren, Scheffer, Ezcurra, Gutiérrez, & Mohren, 2001; Marengo, Tomasella, Alves, Soares, & Rodriguez, 2011). The AMO also influences climate variation at our site and other areas in the region (Elder, Balling, Cerveny, & Krahenbuhl, 2014). Tropical tree recruitment, growth, and mortality all vary among years in relation to such local climate variation, and thus, stand-level productivity and mortality fluxes vary as well.

Extended periods of drier than normal conditions—that is, droughts—are associated with increased mortality and decreased



productivity in many tropical forests (Feldpausch et al., 2016; Phillips et al., 2009). The severe 1982–1983 El Niño made the dry season on BCI longer and harsher than normal, and was associated with higher tree mortality rates. Similarly, many sites in the Amazon and south-east Asia experienced elevated mortality during and after El Niño droughts (e.g., Brando et al., 2014; McDowell et al., 2018; Phillips et al., 2010; Qie et al., 2017; Rowland et al., 2015). El Niño droughts in the Amazon were also associated with decreased leaf area index, decreased photosynthesis (attributed to both stomatal closure and lower leaf area), and decreased woody productivity during the drought periods (Aguilón, Hérault, Burban, Wagner, & Bonal, 2018; Asner, Townsend, & Braswell, 2000; Rowland et al., 2014; Santos et al., 2018). Tree-ring studies generally find that woody productivity is positively correlated with annual precipitation (Alfaro-Sánchez, Muller-Landau, Wright, & Camarero, 2017; Schippers, Sterck, Vlam, & Zuidema, 2015), consistent with the idea that dry years are bad for productivity. Temporal variation in woody growth in relation to water availability could be explained in part by shifts in allocation (rather than simply differences in total GPP and NPP), with trees allocating to increased xylem growth in wet periods after droughts in order to replace drought-damaged xylem (Trugman et al., 2018).

Although most studies have emphasized the negative effects of drier periods, drier years also bring higher solar radiation, and this can lead to more favorable conditions for forest productivity and tree survival if the dryness is not too extreme. On BCI, the drier periods of the 1987–1988 and 1997–1998 El Niños (Figure S18) were associated with elevated fruit production (Detto, Wright, Calderón, & Muller-Landau, 2018), and the 5 year census periods encompassing these events featured above-average woody productivity (this study, Meakem et al., 2017). El Niño events are associated with reduced rainfall during the wet season across northern South American and southern Central America (Ropelewski & Halpert, 1987). Moisture availability remains ample and reduced cloud cover and great solar radiation relieves light limitation (Graham, Mulkey, Kitajima, Phillips, & Wright, 2003), providing a straightforward explanation for observed increases in productivity (Detto et al., 2018; Wright & Calderón, 2006). Consistent with these findings, a previous analysis of multiple moist and wet tropical forests, including BCI, found higher tree growth in census intervals with higher solar radiation (Dong et al., 2012). There are also reasons why dry years might exhibit lower rather than higher mortality. Reduced light limitation in sunnier years might reduce mortality rates for shaded understory tree, and fewer and smaller storms may reduce mortality due to windthrows, lightning, and landslides (Aubry-Kientz, Rossi, Wagner, & Hérault, 2015; Espírito-Santo et al., 2010; Guzzetti, Peruccacci, Rossi, & Stark, 2008; Yanoviak, Gora, Burchfield, Bitzer, & Detto, 2017).

Interannual variation in temperature may also contribute to interannual variation in tropical forest carbon dynamics. Warmer years have been associated with lower tropical tree growth in several studies (Clark, Piper, Keeling, & Clark, 2003; Dong et al., 2012;

Schippers et al., 2015). Temperature directly affects photosynthesis and respiration rates, with photosynthesis responding unimodally to temperature, and respiration increasing continuously with temperature (Lloyd & Farquhar, 2008; Slot & Winter, 2017). Furthermore, high leaf temperatures increase vapor pressure deficits and water demand, leading to stomatal closure, and it is this effect on water relations that appears to be the main contributor to temperature limitation on productivity (Aguilón et al., 2018; Slot & Winter, 2017). Higher atmospheric carbon dioxide concentrations increase plant water use efficiency, and may thereby partly mitigate the negative effects of higher temperatures and drier conditions on productivity (Holtum & Winter, 2010).

In addition to the direct effects of climate on plant physiological function and mortality risk, climate may also influence forest carbon cycles indirectly by causing shifts in allocation, stand structure, functional composition, and influences of interacting species. Plants may increase or decrease allocation to woody growth, including adding to or drawing down carbon stores, depending on past and current climate conditions (Clark, Clark, & Oberbauer, 2013; Doughty et al., 2014; Trugman et al., 2018). Past mortality events from climate alter tree age and size distributions, gap phase distributions, and thereby stand-level carbon budgets (Anderegg, Schwalm, et al., 2015; Chazdon, 2003; Clark, 2007). Differential recruitment, survival, and growth of plant functional types under particular climate conditions also alters functional composition, and thereby the response of forests to future climate. For example, mortality of drought-intolerant species under drought can shift composition toward more drought-tolerant species, with implications for forest carbon budgets and resilience to future droughts (Esquivel-Muelbert et al., 2019; McDowell et al., 2008; Ouédraogo, Mortier, Gourlet-Fleury, Freycon, & Picard, 2013). The proliferation of pathogens and insect herbivores, and thus their effects on trees, is also highly sensitive to climate conditions (Anderegg, Hicke, et al., 2015; Van Bael et al., 2004).

## 4.2 | Detecting and attributing long-term change

Tropical forests are experiencing global atmospheric and climate change. Mean atmospheric CO<sub>2</sub> concentration is increasing continuously, with an increase of 15% over the duration of our study (from 346 ppm in 1985 to 400 ppm in 2015, Figure S18g). Temperatures are increasing in most tropical regions, and precipitation patterns are changing in region-specific ways (Buckley & Huey, 2016; Malhi & Wright, 2004). At our site, the focal 30 year period exhibited trends of +0.15°C per decade in daily maximum temperature, +0.04°C per decade in daily minimum temperature, +5 mm/year in annual precipitation, +0.05% soil moisture per year, and −1.3 W m<sup>−2</sup> year<sup>−1</sup> in annual solar radiation. Trends in annual means of these BCI climate metrics over the 30 year period alone were not statistically significant after Bonferroni correction (individual *p*-values of .075, .44, .66, .033, and .48, respectively), reflecting the relative strength of interannual variation. This interannual variation limits the ability to detect long-term trends—but failure to reject the null hypothesis of

no increase should not be misinterpreted as support for constant climate conditions.

These atmospheric and climate changes are hypothesized to be changing tropical forest carbon dynamics (Lewis, Malhi, & Phillips, 2004). CO<sub>2</sub> is needed for photosynthesis, and physiological models suggest that the observed increase in CO<sub>2</sub> should increase growth (Phillips & Lewis, 2014), although there is uncertainty about the degree to which growth responses are limited by availability of other nutrients, and within-plant carbon demands (Körner, 2009, 2003b; Wright et al., 2011). Spatial variation in climate among tropical forests is associated with variation in tropical forest carbon stocks and fluxes (Álvarez-Dávila et al., 2017; Becknell, Kissing Kucek, & Powers, 2012; Poorter et al., 2016; Taylor et al., 2017), suggesting that directional climate changes should also change forest carbon budgets in the long term. As discussed above, tropical forests are also sensitive to temporal variation in climate conditions, further suggesting that climate change will matter. However, the relationship of short-term to long-term climate responses is not straightforward, because the importance of particular mechanisms shifts with the timescale. Allocational shifts to/from woody productivity, reproductive output, and carbohydrate stores play a large role in variation over seasonal to annual time scales (Dickman et al., 2018; Doughty et al., 2014), but are likely to play little role at decadal and longer time scales. In contrast, shifts in functional composition of the tree community are likely to play a large role in responses to long-term climate variation (van der Sande et al., 2016), but very little role in short-term responses. Such compositional shifts are in general expected to decrease the sensitivity of forest carbon fluxes to climate variation, as the forest becomes increasingly dominated by species that do relatively well in the new climate conditions (Esquivel-Muelbert et al., 2019; Fauset et al., 2015; Feldpausch et al., 2016).

However, evidence of long-term changes in tropical forest carbon cycling is mixed, with divergent patterns across studies. Increasing woody productivity and mortality were found in analyses of the RAINFOR network of Amazonian plots (Brienen et al., 2015), but not in site-specific studies of BCI (this study) or La Selva (Clark, Asao, et al., 2017; Clark et al., 2013; Clark, Clark, et al., 2017). On average, studies report increased biomass densities in old-growth tropical forests (Brienen et al., 2015; Chave et al., 2008, Lewis et al., 2009; Muller-Landau et al., 2014; Qie et al., 2017; Rutishauser, Wagner, Herault, Nicolini, & Blanc, 2010), but this pattern too is not universal (this study, Chave et al., 2008; Clark, Clark, et al., 2017; Feeley et al., 2007) and the causes of observed increases continue to be debated (Clark, 2004; Lewis et al., 2009; Muller-Landau, 2009; Wright, 2013). It is notable that two of the most intensive long-term studies of focal sites, this 30 year study of BCI and Clark, Clark, et al. (2017)'s 40 year study of La Selva, find multidecadal stability in forest structure and dynamics, in striking contrast to the "Bigger and Faster" hypothesis.

The large uncertainty surrounding estimated fluxes and their long-term trends observed here, even with such a large-scale long-term study, highlights the difficulty of accurately capturing

changes in forest dynamics from field data (Clark, Asao, et al., 2017). Wagner, Rutishauser, Blanc, and Herault (2010) calculated that estimating even the mean EAGB loss within 20% error with 95% confidence in a particular forest would require ~200 ha-years of monitoring, far more than the usual size and duration of most forest monitoring experiments. The effort required to accurately estimate a long-term trend is much higher still—even a trend as large as 1% a year amounts to only 10% a decade, within the error limits of the Wagner et al. (2010) calculation. Detection of long-term trends is further complicated by sensitivity of estimated trends to the precise methods of data quality assessment and quality control (QAQC; Figure S18). Many common QAQC procedures result in systematic biases in whole-plot statistics (Cushman et al., 2014; Muller-Landau et al., 2014). Our analysis followed current best practices for calculating EAGB fluxes, including standardizing effective POM (Cushman et al., 2014) and avoiding data "cleaning" procedures that can systematically bias whole-plot statistics (Muller-Landau et al., 2014).

#### 4.3 | Conclusion and future directions

The tropical forest on BCI exhibited large temporal variability in stand-level productivity and mortality fluxes over 30 years, even after controlling for disturbance-recovery dynamics, but no long-term trend. Observed temporal variability was aligned to some degree with ENSO-related climate variation, but with a markedly different pattern than is usually reported, highlighting the complexity of tropical forest climate responses. While the drier conditions of El Niño events have been associated with increased tree mortality and reduced productivity in the Amazon (Feldpausch et al., 2016; Lewis, Brando, Phillips, Heijden, & Nepstad, 2011), the drier and sunnier conditions during El Niño events were associated with enhanced productivity and no change in mortality on BCI (Detto et al., 2018; Meakem et al., 2017). No long-term directional trend in productivity, mortality, or biomass was evident in our data, but such a trend could well be obscured by the strong interannual variation.

A better understanding of tropical forest responses to climate variation and long-term trends requires both more data and integration with mechanistic models. Although climate and atmospheric change is global, climate effects are locally variable, and forest responses are dependent on a myriad of other local factors, including species composition and disturbance history, resulting in highly variable EAGB dynamics (Clark et al., 2013). Future multisite analyses of large plot datasets using the methods developed here could provide insights into temporal and spatial variation in tropical forest carbon fluxes (Chave et al., 2008; van der Sande et al., 2016; Wagner et al., 2016). However, any studies based on extant plot datasets are likely to fall short of what is needed to quantify overall trends given high temporal and spatial variability, and the nonsystematic placement of sampling plots (Marvin et al., 2014; McMichael et al., 2017; Saatchi et al., 2015; Wright, 2006). Improvements in remote sensing ultimately promise more comprehensive and consistent measurements of tropical forest structure

and function, and their change over time (Bastin et al., 2018; Rödig et al., 2018; Saatchi et al., 2011), although the contribution of recovery from past disturbances remains to be resolved (McMichael et al., 2017; Palace et al., 2017). Studies integrating mechanistic models with data on climate drivers and forest dynamics are uniquely well suited to glean insights into the ultimate mechanisms behind observed patterns and to disentangling the roles of temperature, rainfall, atmospheric carbon dioxide, soils, species composition, and site history (Levine et al., 2016; Schippers et al., 2015).

## ACKNOWLEDGEMENTS

E.R. and S.J.D. were supported by the Next Generation Ecosystem Experiments-Tropics, funded by the US Department of Energy, Office of Science, Office of Biological and Environmental Research. We gratefully acknowledge the contributions to the Barro Colorado Island 50 ha plot of Robin Foster, co-founder of the plot; Rolando Pérez and Salomón Aguilar for species identification; Suzanne Lao for data management; Steven Dolins for database design; and hundreds of field-workers over the years. The BCI forest dynamics plot dataset was made possible by the financial support of the National Science Foundation, the Smithsonian Tropical Research Institute, and the MacArthur Foundation. We thank Deborah A. Clark and an anonymous reviewer for constructive comments on this manuscript.

## CONFLICT OF INTEREST

All authors declare no conflict of interest.

## ORCID

Ervan Rutishauser  <https://orcid.org/0000-0003-1182-4032>

## REFERENCES

- Aguilos, M., Hérault, B., Burban, B., Wagner, F., & Bonal, D. (2018). What drives long-term variations in carbon flux and balance in a tropical rainforest in French Guiana? *Agricultural & Forest Meteorology*, 253–254, 114–123. <https://doi.org/10.1016/j.agrformet.2018.02.009>
- Alfaro-Sánchez, R., Muller-Landau, H. C., Wright, S. J., & Camarero, J. J. (2017). Growth and reproduction respond differently to climate in three Neotropical tree species. *Oecologia*, 184, 531–541. <https://doi.org/10.1007/s00442-017-3879-3>
- Álvarez-Dávila, E., Cayuela, L., González-Caro, S., Aldana, A. M., Stevenson, P. R., Phillips, O., ... Rey-Benayas, J. M. (2017). Forest biomass density across large climate gradients in northern South America is related to water availability but not with temperature. *PLoS ONE*, 12(3), e0171072. <https://doi.org/10.1371/journal.pone.0171072>
- Anderegg, W. R. L., Hicke, J. A., Fisher, R. A., Allen, C. D., Aukema, J., Bentz, B., ... Zeppel, M. (2015). Tree mortality from drought, insects, and their interactions in a changing climate. *New Phytologist*, 208, 674–683. <https://doi.org/10.1111/nph.13477>
- Anderegg, W. R. L., Schwalm, C., Biondi, F., Camarero, J. J., Koch, G., Litvak, M., ... Pacala, S. (2015). Pervasive drought legacies in forest ecosystems and their implications for carbon cycle models. *Science*, 349, 528–532. <https://doi.org/10.1126/science.aab1833>
- Asner, G. P., Townsend, A. R., & Braswell, B. H. (2000). Satellite observation of El Niño effects on Amazon Forest phenology and productivity. *Geophysical Research Letters*, 27, 981–984. <https://doi.org/10.1029/1999GL011113>
- Aubry-Kientz, M., Rossi, V., Wagner, F., & Hérault, B. (2015). Identifying climatic drivers of tropical forest dynamics. *Biogeosciences*, 12, 5583–5596. <https://doi.org/10.5194/bg-12-5583-2015>
- Baker, T. R., Phillips, O. L., Malhi, Y., Almeida, S., Arroyo, L., Di Fiore, A., ... Vasquez Martinez, R. (2004). Increasing biomass in Amazonian forest plots. *Philosophical Transactions of the Royal Society of London. Series B: Biological Sciences*, 359, 353–365. <https://doi.org/10.1098/rstb.2003.1422>
- Baskerville, G. (1972). Use of logarithmic regression in the estimation of plant biomass. *Canadian Journal of Forest Research*, 2, 49–53. <https://doi.org/10.1139/x72-009>
- Bastin, J.-F., Rutishauser, E., Kellner, J. R., Saatchi, S., Pélissier, R., Hérault, B., ... Zebaze, D. (2018). Pan-tropical prediction of forest structure from the largest trees. *Global Ecology and Biogeography*, 27, 1366–1383. <https://doi.org/10.1111/geb.12803>
- Bates, D., Mächler, M., Bolker, B., & Walker, S. (2015). Fitting linear mixed-effects models using lme4. *Journal of Statistical Software*, 67(1), 1–48. <https://doi.org/10.18637/jss.v067.i01>
- Becknell, J. M., Kissing Kucek, L., & Powers, J. S. (2012). Aboveground biomass in mature and secondary seasonally dry tropical forests: A literature review and global synthesis. *Forest Ecology and Management*, 276, 88–95.
- Bormann, F. H., & Likens, G. E. (1979). *Pattern and process in a forested ecosystem: Disturbance, development and the steady state based on the Hubbard Brook Ecosystem Study* (1st ed.). New York, NY: Springer-Verlag.
- Brando, P. M., Balch, J. K., Nepstad, D. C., Morton, D. C., Putz, F. E., Coe, M. T., ... Soares-Filho, B. S. (2014). Abrupt increases in Amazonian tree mortality due to drought-fire interactions. *Proceedings of the National Academy of Sciences of the United States of America*, 111, 6347–6352. <https://doi.org/10.1073/pnas.1305499111>
- Brienen, R. J. W., Phillips, O. L., Feldpausch, T. R., Gloor, E., Baker, T. R., Lloyd, J., ... Zagt, R. J. (2015). Long-term decline of the Amazon carbon sink. *Nature*, 519, 344–348. <https://doi.org/10.1038/nature14283>
- Brcic, T. M., Willis, K. J., Harris, D. J., & Washington, R. (2006). Culture or climate? The relative influences of past processes on the composition of the lowland Congo rainforest. *Philosophical Transactions of the Royal Society B: Biological Sciences*, 362, 229–242. <https://doi.org/10.1098/rstb.2006.1982>
- Buckley, L. B., & Huey, R. B. (2016). Temperature extremes: Geographic patterns, recent changes, and implications for organismal vulnerabilities. *Global Change Biology*, 22, 3829–3842. <https://doi.org/10.1111/gcb.13313>
- Chave, J., Condit, R., Muller-Landau, H. C., Thomas, S. C., Ashton, P. S., Bunyavechewin, S., ... Losos, E. C. (2008). Assessing evidence for a pervasive alteration in tropical tree communities. *PLoS Biology*, 6, 455–462. <https://doi.org/10.1371/journal.pbio.0060045>
- Chave, J., Réjou-Méchain, M., Búrquez, A., Chidumayo, E., Colgan, M. S., Delitti, W. B., ... Vieilledent, G. (2014). Improved allometric models to estimate the aboveground biomass of tropical trees. *Global Change Biology*, 20, 3177–3190. <https://doi.org/10.1111/gcb.12629>
- Chazdon, R. L. (2003). Tropical forest recovery: Legacies of human impact and natural disturbances. *Perspectives in Plant Ecology, Evolution and Systematics*, 6, 51–71. <https://doi.org/10.1078/1433-8319-00042>
- Clark, D. (2004). Sources or sinks? The responses of tropical forests to current and future climate and atmospheric composition. *Philosophical*

- Transactions of the Royal Society of London. Series B: Biological Sciences*, 359, 477–491. <https://doi.org/10.1098/rstb.2003.1426>
- Clark, D. A. (2007). Detecting tropical forests' responses to global climatic and atmospheric change: Current challenges and a way forward. *Biotropica*, 39, 4–19. <https://doi.org/10.1111/j.1744-7429.2006.00227.x>
- Clark, D. A., Asao, S., Fisher, R., Reed, S., Reich, P. B., Ryan, M. G., ... Yang, X. (2017). Field data to benchmark the carbon cycle models for tropical forests. *Biogeosciences*, 14(20), 4663–4690. <https://doi.org/10.5194/bg-14-4663-2017>
- Clark, D. A., Clark, D. B., & Oberbauer, S. F. (2013). Field-quantified responses of tropical rainforest aboveground productivity to increasing CO<sub>2</sub> and climatic stress, 1997–2009: Tropical rainforest productivity responses. *Journal of Geophysical Research: Biogeosciences*, 118, 783–794. <https://doi.org/10.1002/jgrg.20067>
- Clark, D. B., Clark, D. A., Oberbauer, S. F., & Kellner, J. R. (2017). Multidecadal stability in tropical rain forest structure and dynamics across an old-growth landscape. *PLoS ONE*, 12, e0183819. <https://doi.org/10.1371/journal.pone.0183819>
- Clark, D. A., Piper, S. C., Keeling, C. D., & Clark, D. B. (2003). Tropical rain forest tree growth and atmospheric carbon dynamics linked to interannual temperature variation during 1984–2000. *Proceedings of the National Academy of Sciences of the United States of America*, 100, 5852–5857. <https://doi.org/10.1073/pnas.0935903100>
- Condit, R. (1998). *Tropical forest census plots: Methods and results from Barro Colorado Island, Panama and a comparison with other plots*. Berlin, Germany: Springer Science & Business Media.
- Condit, R., Hubbell, S. P., & Foster, R. B. (1996). Changes in tree species abundance in a Neotropical forest: Impact of climate change. *Journal of Tropical Ecology*, 12, 231–256. <https://doi.org/10.1017/S0266467400009433>
- Cushman, K. C., Muller-Landau, H. C., Condit, R. S., & Hubbell, S. P. (2014). Improving estimates of biomass change in buttressed trees using tree taper models. *Methods in Ecology and Evolution*, 5, 573–582. <https://doi.org/10.1111/2041-210X.12187>
- Denslow, J. S., Ellison, A. M., & Sanford, R. E. (1998). Treefall gap size effects on above- and below-ground processes in a tropical wet forest. *Journal of Ecology*, 86, 597–609. <https://doi.org/10.1046/j.1365-2745.1998.00295.x>
- Detto, M., Wright, S. J., Calderón, O., & Muller-Landau, H. C. (2018). Resource acquisition and reproductive strategies of tropical forest in response to the El Niño–Southern Oscillation. *Nature Communications*, 9, 913. <https://doi.org/10.1038/s41467-018-03306-9>
- Dickman, L. T., McDowell, N. G., Grossiord, C., Collins, A. D., Wolfe, B. T., Detto, M., ... Chambers, J. Q. (2018). Homeostatic maintenance of nonstructural carbohydrates during the 2015–2016 El Niño drought across a tropical forest precipitation gradient. *Plant, Cell and Environment*, 42(5), 1705–1714. <https://doi.org/10.1111/pce.13501>
- Dong, S. X., Davies, S. J., Ashton, P. S., Bunyavejchewin, S., Supardi, M. N., Kassim, A. R., ... Moorcroft, P. R. (2012). Variability in solar radiation and temperature explains observed patterns and trends in tree growth rates across four tropical forests. *Proceedings of the Royal Society B: Biological Sciences*, 279, 3923–3931. <https://doi.org/10.1098/rspb.2012.1124>
- dos Santos, V. A. H. F., Ferreira, M. J., Rodrigues, J. V. F. C., Garcia, M. N., Ceron, J. V. B., Nelson, B. W., & Saleska, S. R. (2018). Causes of reduced leaf-level photosynthesis during strong El Niño drought in a Central Amazon forest. *Global Change Biology*, 24, 4266–4279. <https://doi.org/10.1111/gcb.14293>
- Doughty, C. E., Malhi, Y., Araujo-Murakami, A., Metcalfe, D. B., Silva-Espejo, J. E., Arroyo, L., ... Ledezma, R. (2014). Allocation trade-offs dominate the response of tropical forest growth to seasonal and interannual drought. *Ecology*, 95, 2192–2201. <https://doi.org/10.1890/13-1507.1>
- Doughty, C. E., Metcalfe, D. B., Girardin, C. A. J., Amézquita, F. F., Cabrera, D. G., Huasco, W. H., ... Malhi, Y. (2015). Drought impact on forest carbon dynamics and fluxes in Amazonia. *Nature*, 519, 78–82. <https://doi.org/10.1038/nature14213>
- Elder, R. C., Balling, R. C., Cerveny, R. S., & Krahenbuhl, D. (2014). Regional variability in drought as a function of the Atlantic Multidecadal Oscillation. *Caribbean Journal of Science*, 48, 31–44. <https://doi.org/10.18475/cjos.v48i1.a5>
- Espirito-Santo, F. D. B., Gloor, M., Keller, M., Malhi, Y., Saatchi, S., Nelson, B., ... Phillips, O. L. (2014). Size and frequency of natural forest disturbances and the Amazon forest carbon balance. *Nature Communications*, 5, 3434. <https://doi.org/10.1038/ncomms4434>
- Espirito-Santo, F. D. B., Keller, M., Braswell, B., Nelson, B. W., Frohling, S., & Vicente, G. (2010). Storm intensity and old-growth forest disturbances in the Amazon region. *Geophysical Research Letters*, 37, L11403. <https://doi.org/10.1029/2010gl043146>
- Esquivel-Muelbert, A., Baker, T. R., Dexter, K. G., Lewis, S. L., Brien, R. J. W., Feldpausch, T. R., ... Phillips, O. L. (2019). Compositional response of Amazon forests to climate change. *Global Change Biology*, 25, 39–56. <https://doi.org/10.1111/gcb.14413>
- Fauset, S., Johnson, M. O., Gloor, M., Baker, T. R., Monteagudo, A. M., Brien, R. J. W., ... Phillips, O. L. (2015). Hyperdominance in Amazonian forest carbon cycling. *Nature Communications*, 6, 6857. <https://doi.org/10.1038/ncomms7857>
- Feeley, K. J., Wright, J., Supardi, N., Kassim, A. R., & Davies, S. J. (2007). Decelerating growth in tropical forest trees. *Ecology Letters*, 10, 461–469. <https://doi.org/10.1111/j.1461-0248.2007.01033.x>
- Feldpausch, T. R., Phillips, O. L., Brien, R. J. W., Gloor, E., Lloyd, J., Lopez-Gonzalez, G., ... Dávila, E. Á. (2016). Amazon forest response to repeated droughts. *Global Biogeochemical Cycles*, 30, 964–982. <https://doi.org/10.1002/2015GB005133>
- Fisher, J. I., Hurr, G. C., Thomas, R. Q., & Chambers, J. Q. (2008). Clustered disturbances lead to bias in large-scale estimates based on forest sample plots. *Ecology Letters*, 11, 554–563. <https://doi.org/10.1111/j.1461-0248.2008.01169.x>
- Goodman, R. C., Phillips, O. L., del Castillo Torres, D., Freitas, L., Cortese, S. T., Monteagudo, A., & Baker, T. R. (2013). Amazon palm biomass and allometry. *Forest Ecology and Management*, 310, 994–1004. <https://doi.org/10.1016/j.foreco.2013.09.045>
- Graham, E. A., Mulkey, S. S., Kitajima, K., Phillips, N. G., & Wright, S. J. (2003). Cloud cover limits net CO<sub>2</sub> uptake and growth of a rainforest tree during tropical rainy seasons. *Proceedings of the National Academy of Sciences of the United States of America*, 100, 572–576. <https://doi.org/10.1073/pnas.0133045100>
- Guzzetti, F., Peruccacci, S., Rossi, M., & Stark, C. P. (2008). The rainfall intensity–duration control of shallow landslides and debris flows: An update. *Landslides*, 5, 3–17. <https://doi.org/10.1007/s10346-007-0112-1>
- Harms, K. E., Condit, R., Hubbell, S. P., & Foster, R. B. (2001). Habitat associations of trees and shrubs in a 50-ha Neotropical forest plot. *Journal of Ecology*, 89, 947–959. <https://doi.org/10.1046/j.0022-0477.2001.00615.x>
- Holmgren, M., Scheffer, M., Ezcurra, E., Gutiérrez, J. R., & Mohren, G. M. J. (2001). El Niño effects on the dynamics of terrestrial ecosystems. *Trends in Ecology & Evolution*, 16, 89–94. [https://doi.org/10.1016/S0169-5347\(00\)02052-8](https://doi.org/10.1016/S0169-5347(00)02052-8)
- Holtum, J. A., & Winter, K. (2010). Elevated [CO<sub>2</sub>] and forest vegetation: More a water issue than a carbon issue? *Functional Plant Biology*, 37, 694–702. <https://doi.org/10.1071/FP10001>
- Hubbell, S. P., Foster, R. B., O'Brien, S. T., Harms, K. E., Condit, R., Wechsler, B., ... De Lao, S. L. (1999). Light-gap disturbances, recruitment limitation, and tree diversity in a neotropical forest. *Science*, 283, 554–557. <https://doi.org/10.1126/science.283.5401.554>
- Kohyama, T. S., Kohyama, T. I., & Sheil, D. (2019). Estimating net biomass production and loss from repeated measurements of trees in forests



- and woodlands: Formulae, biases and recommendations. *Forest Ecology and Management*, 433, 729–740. <https://doi.org/10.1016/j.foreco.2018.11.010>
- Körner, C. (2003a). Slow in, rapid out – Carbon flux studies and Kyoto targets. *Science*, 300, 1242–1243. <https://doi.org/10.1126/science.1084460>
- Körner, C. (2003b). Carbon limitation in trees. *Journal of Ecology*, 91, 4–17. <https://doi.org/10.1046/j.1365-2745.2003.00742.x>
- Körner, C. (2009). Responses of humid tropical trees to rising CO<sub>2</sub>. *Annual Review of Ecology Evolution and Systematics*, 40, 61–79. <https://doi.org/10.1146/annurev.ecolsys.110308.120217>
- Körner, C. (2015). Paradigm shift in plant growth control. *Current Opinion in Plant Biology*, 25, 107–114. <https://doi.org/10.1016/j.pbi.2015.05.003>
- Levine, N. M., Zhang, K., Longo, M., Baccini, A., Phillips, O. L., Lewis, S. L., ... Moorcroft, P. R. (2016). Ecosystem heterogeneity determines the ecological resilience of the Amazon to climate change. *Proceedings of the National Academy of Sciences of the United States of America*, 113, 793–797. <https://doi.org/10.1073/pnas.1511344112>
- Levis, C., Costa, F. R. C., Bongers, F., Peña-Claros, M., Clement, C. R., Junqueira, A. B., ... Ter Steege, H. (2017). Persistent effects of pre-Columbian plant domestication on Amazonian forest composition. *Science*, 355, 925–931. <https://doi.org/10.1126/science.aal0157>
- Lewis, S. L., Brando, P. M., Phillips, O. L., van der Heijden, G. M. F., & Nepstad, D. (2011). The 2010 Amazon drought. *Science*, 331, 554. <https://doi.org/10.1126/science.1200807>
- Lewis, S. L., Lloyd, J., Sitch, S., Mitchard, E. T. A., & Laurance, W. F. (2009). Changing ecology of tropical forests: Evidence and drivers. *Annual Review of Ecology, Evolution, and Systematics*, 40, 529–549. <https://doi.org/10.1146/annurev.ecolsys.39.110707.173345>
- Lewis, S. L., Malhi, Y., & Phillips, O. L. (2004). Fingerprinting the impacts of global change on tropical forests. *Philosophical Transactions of the Royal Society B: Biological Sciences*, 359, 437–462. <https://doi.org/10.1098/rstb.2003.1432>
- Lewis, S. L., Sonke, B., Sunderland, T., Begne, S. K., Lopez-Gonzalez, G., van der Heijden, G. M. F., ... Zemagho, L. (2013). Above-ground biomass and structure of 260 African tropical forests. *Philosophical Transactions of the Royal Society B: Biological Sciences*, 368, 20120295–20120295. <https://doi.org/10.1098/rstb.2012.0295>
- Liu, J., Bowman, K. W., Schimel, D. S., Parazoo, N. C., Jiang, Z., Lee, M., ... Elderling, A. (2017). Contrasting carbon cycle responses of the tropical continents to the 2015–2016 El Niño. *Science*, 358, eaam5690. <https://doi.org/10.1126/science.aam5690>
- Lloyd, J., & Farquhar, G. D. (2008). Effects of rising temperatures and [CO<sub>2</sub>] on the physiology of tropical forest trees. *Philosophical Transactions of the Royal Society B: Biological Sciences*, 363, 1811–1817. <https://doi.org/10.1098/rstb.2007.0032>
- Loader, C. (1999). *Local regression and likelihood*. New York, NY: Springer Science & Business Media.
- Magnabosco Marra, D., Trumbore, S. E., Higuchi, N., Ribeiro, G. H. P. M., Negrón-Juárez, R. I., Holzwarth, F., ... Wirth, C. (2018). Windthrows control biomass patterns and functional composition of Amazon forests. *Global Change Biology*, 24, 5867–5881. <https://doi.org/10.1111/gcb.14457>
- Malhi, Y., & Wright, J. (2004). Spatial patterns and recent trends in the climate of tropical rainforest regions. *Philosophical Transactions of the Royal Society of London. Series B: Biological Sciences*, 359, 311–329. <https://doi.org/10.1098/rstb.2003.1433>
- Marengo, J. A., Tomasella, J., Alves, L. M., Soares, W. R., & Rodriguez, D. A. (2011). The drought of 2010 in the context of historical droughts in the Amazon region. *Geophysical Research Letters*, 38. <https://doi.org/10.1029/2011GL047436>
- Marvin, D. C., Asner, G. P., Knapp, D. E., Anderson, C. B., Martin, R. E., Sinca, F., & Tupayachi, R. (2014). Amazonian landscapes and the bias in field studies of forest structure and biomass. *Proceedings of the National Academy of Sciences of the United States of America*, 111, E5224–E5232. <https://doi.org/10.1073/pnas.1412999111>
- Mayle, F. E., Burbridge, R., & Killeen, T. J. (2000). Millennial-scale dynamics of southern Amazonian Rain Forests. *Science*, 290, 2291–2294. <https://doi.org/10.1126/science.290.5500.2291>
- McDowell, N., Allen, C. D., Anderson-Teixeira, K., Brando, P., Brien, R., Chambers, J., ... Xu, X. (2018). Drivers and mechanisms of tree mortality in moist tropical forests. *New Phytologist*, 219, 851–869. <https://doi.org/10.1111/nph.15027>
- McDowell, N., Pockman, W. T., Allen, C. D., Breshears, D. D., Cobb, N., Kolb, T., ... Yepez, E. A. (2008). Mechanisms of plant survival and mortality during drought: Why do some plants survive while others succumb to drought? *New Phytologist*, 178, 719–739. <https://doi.org/10.1111/j.1469-8137.2008.02436.x>
- McMichael, C. N. H., Matthews-Bird, F., Farfan-Rios, W., & Feeley, K. J. (2017). Ancient human disturbances may be skewing our understanding of Amazonian forests. *Proceedings of the National Academy of Sciences of the United States of America*, 114, 522–527. <https://doi.org/10.1073/pnas.1614577114>
- Meakem, V., Tepley, A. J., Gonzalez-Akre, E. B., Herrmann, V., Muller-Landau, H. C., Wright, S. J., ... Anderson-Teixeira, K. J. (2017). Role of tree size in moist tropical forest carbon cycling and water deficit responses. *New Phytologist*, 219, 947–958. <https://doi.org/10.1111/nph.14633>
- Muller-Landau, H. C. (2009). Carbon cycle: Sink in the African jungle. *Nature*, 457, 969–970. <https://doi.org/10.1038/457969a>
- Muller-Landau, H. C., Detto, M., Chisholm, R. A., Hubbell, S. P., & Condit, R. (2014). Detecting and projecting changes in forest biomass from plot data. In D. A. Coomes, D. F. R. P. Burslem, & W. D. Simonson (Eds.), *Forests and global change, ecological review* (pp. 381–416). Cambridge, UK: Cambridge University Press.
- Oslisly, R., White, L., Bentele, I., Favier, C., Fontugne, M., Gillet, J.-F., & Sebag, D. (2013). Climatic and cultural changes in the west Congo Basin forests over the past 5000 years. *Philosophical Transactions of the Royal Society B: Biological Sciences*, 368, 20120304. <https://doi.org/10.1098/rstb.2012.0304>
- Quédraogo, D.-Y., Mortier, F., Gourlet-Fleury, S., Freycon, V., & Picard, N. (2013). Slow-growing species cope best with drought: Evidence from long-term measurements in a tropical semi-deciduous moist forest of Central Africa. *Journal of Ecology*, 101, 1459–1470. <https://doi.org/10.1111/1365-2745.12165>
- Palace, M. W., McMichael, C. N. H., Braswell, B. H., Hagen, S. C., Bush, M. B., Neves, E., ... Frolking, S. (2017). Ancient Amazonian populations left lasting impacts on forest structure. *Ecosphere*, 8, e02035. <https://doi.org/10.1002/ecs2.2035>
- Paton, S. (2018). *2017 Meteorological and hydrological summary for Barro Colorado Island*. Balboa, Panama: Smithsonian Tropical Research Institute.
- Phillips, O. L., Aragao, L. E. O. C., Lewis, S. L., Fisher, J. B., Lloyd, J., Lopez-Gonzalez, G., ... Torres-Lezama, A. (2009). Drought sensitivity of the Amazon Rainforest. *Science*, 323, 1344–1347. <https://doi.org/10.1126/science.1164033>
- Phillips, O. L., & Lewis, S. L. (2014). Recent changes in tropical forest biomass and dynamics. In D. A. Coomes, D. F. R. P. Burslem, & W. D. Simonson (Eds.), *Forests and global change, ecological review* (pp. 77–108). Cambridge, UK: Cambridge University Press.
- Phillips, O. L., Malhi, Y., Higuchi, N., Laurance, W., Nunez, P. V., Vasquez, R. M., ... Grace, J. (1998). Changes in the carbon balance of tropical forest: Evidence from long-term plots. *Science*, 282, 439–442. <https://doi.org/10.1126/science.282.5388.439>
- Phillips, O. L., van der Heijden, G., Lewis, S. L., López-González, G., Aragão, L. E. O. C., Lloyd, J., ... Vilanova, E. (2010). Drought-mortality relationships for tropical forests. *New Phytologist*, 187, 631–646. <https://doi.org/10.1111/j.1469-8137.2010.03359.x>
- Poorter, L., Bongers, F., Aide, T. M., Almeyda Zambrano, A. M., Balvanera, P., Becknell, J. M., ... Rozendaal, D. M. A. (2016). Biomass resilience of

- Neotropical secondary forests. *Nature*, 530(7589), 211–214. <https://doi.org/10.1038/nature16512>
- Qie, L., Lewis, S. L., Sullivan, M. J. P., Lopez-Gonzalez, G., Pickavance, G. C., Sunderland, T., ... Phillips, O. L. (2017). Long-term carbon sink in Borneo's forests halted by drought and vulnerable to edge effects. *Nature Communications*, 8(1), 1966. <https://doi.org/10.1038/s41467-017-01997-0>
- Rödig, E., Cuntz, M., Rammig, A., Fischer, R., Taubert, F., & Huth, A. (2018). The importance of forest structure for carbon flux estimates in the Amazon rainforest. *Environmental Research Letters*, 13, 054013. <https://doi.org/10.1088/1748-9326/aabc61>
- Ropelewski, C. F., & Halpert, M. S. (1987). Global and regional scale precipitation patterns associated with the El Niño/Southern Oscillation. *Monthly Weather Review*, 115, 1606–1626. [https://doi.org/10.1175/1520-0493\(1987\)115<1606:GARSPP>2.0.CO;2](https://doi.org/10.1175/1520-0493(1987)115<1606:GARSPP>2.0.CO;2)
- Rowland, L., Lobo-do-Vale, R. L., Christoffersen, B. O., Melém, E. A., Kruijt, B., Vasconcelos, S. S., ... Meir, P. (2015). After more than a decade of soil moisture deficit, tropical rainforest trees maintain photosynthetic capacity, despite increased leaf respiration. *Global Change Biology*, 21, 4662–4672. <https://doi.org/10.1111/gcb.13035>
- Rowland, L., Malhi, Y., Silva-Espejo, J. E., Farfán-Amézquita, F., Halladay, K., Doughty, C. E., ... Phillips, O. L. (2014). The sensitivity of wood production to seasonal and interannual variations in climate in a lowland Amazonian rainforest. *Oecologia*, 174, 295–306. <https://doi.org/10.1007/s00442-013-2766-9>
- Rutishauser, E., Wagner, F., Hérault, B., Nicolini, E. A., & Blanc, L. (2010). Contrasting above-ground biomass balance in a Neotropical rain forest. *Journal of Vegetation Science*, 21, 672–682. <https://doi.org/10.1111/j.1654-1103.2010.01175.x>
- Saatchi, S. S., Harris, N. L., Brown, S., Lefsky, M., Mitchard, E. T. A., Salas, W., ... Morel, A. (2011). Benchmark map of forest carbon stocks in tropical regions across three continents. *Proceedings of the National Academy of Sciences of the United States of America*, 108, 9899–9904. <https://doi.org/10.1073/pnas.1019576108>
- Saatchi, S., Mascaró, J., Xu, L., Keller, M., Yang, Y., Duffy, P., ... Schimel, D. (2015). Seeing the forest beyond the trees. *Global Ecology and Biogeography*, 24, 606–610. <https://doi.org/10.1111/geb.12256>
- Schippers, P., Sterck, F., Vlam, M., & Zuidema, P. A. (2015). Tree growth variation in the tropical forest: Understanding effects of temperature, rainfall and CO<sub>2</sub>. *Global Change Biology*, 21, 2749–2761. <https://doi.org/10.1111/gcb.12877>
- Slot, M., & Winter, K. (2017). In situ temperature relationships of biochemical and stomatal controls of photosynthesis in four lowland tropical tree species. *Plant, Cell and Environment*, 40, 3055–3068. <https://doi.org/10.1111/pce.13071>
- Taylor, P. G., Cleveland, C. C., Wieder, W. R., Sullivan, B. W., Doughty, C. E., Dobrowski, S. Z., & Townsend, A. R. (2017). Temperature and rainfall interact to control carbon cycling in tropical forests. *Ecology Letters*, 20(6), 779–788. <https://doi.org/10.1111/ele.12765>
- Trugman, A. T., Detto, M., Bartlett, M. K., Medvigy, D., Anderegg, W. R. L., Schwalm, C., ... Pacala, S. W. (2018). Tree carbon allocation explains forest drought-kill and recovery patterns. *Ecology Letters*, 21, 1552–1560. <https://doi.org/10.1111/ele.13136>
- Van Bael, S. A., Aiello, A., Valderrama, A., Medianero, E., Samaniego, M., & Wright, S. J. (2004). General herbivore outbreak following an El Niño-related drought in a lowland Panamanian forest. *Journal of Tropical Ecology*, 20, 625–633. <https://doi.org/10.1017/s0266467404001725>
- van der Sande, M. T., Arets, E. J. M. M., Peña-Claros, M., de Avila, A. L., Roopsind, A., Mazzei, L., ... Poorter, L. (2016). Old-growth Neotropical forests are shifting in species and trait composition. *Ecological Monographs*, 86, 228–243. <https://doi.org/10.1890/15-1815.1>
- Wagner, F. H., Hérault, B., Bonal, D., Stahl, C., Anderson, L. O., Baker, T. R., ... Aragão, L. E. O. C. (2016). Climate seasonality limits leaf carbon assimilation and wood productivity in tropical forests. *Biogeosciences*, 13, 2537–2562. <https://doi.org/10.5194/bg-13-2537-2016>
- Wagner, F., Rutishauser, E., Blanc, L., & Hérault, B. (2010). Assessing effects of plot size and census interval on estimates of tropical forest structure and dynamics. *Biotropica*, 42, 664–671. <https://doi.org/10.1111/j.1744-7429.2010.00644.x>
- Watt, A. S. (1947). Pattern and process in plant ecology. *Journal of Ecology*, 35, 1–22.
- Whitmore, T. C. (1989). Canopy gaps and the two major groups of forest trees. *Ecology*, 70, 536–538. <https://doi.org/10.2307/1940195>
- Wright, S. J. (2006). Response to Lewis et al.: The uncertain response of tropical forests to global change. *Trends in Ecology & Evolution*, 21(4), 174–175. <https://doi.org/10.1016/j.tree.2006.02.003>
- Wright, S. J. (2010). The future of tropical forests. *Annals of the New York Academy of Sciences*, 1195, 1–27. <https://doi.org/10.1111/j.1749-6632.2010.05455.x>
- Wright, S. J. (2013). The carbon sink in intact tropical forests. *Global Change Biology*, 19(2), 337–339. <https://doi.org/10.1111/gcb.12052>
- Wright, S. J., & Calderón, O. (2006). Seasonal, El Niño and longer term changes in flower and seed production in a moist tropical forest. *Ecology Letters*, 9, 35–44. <https://doi.org/10.1111/j.1461-0248.2005.00851.x>
- Wright, S. J., Kitajima, K., Kraft, N. J. B., Reich, P. B., Wright, I. J., Bunker, D. E., ... Zanne, A. E. (2010). Functional traits and the growth-mortality trade-off in tropical trees. *Ecology*, 91, 3664–3674. <https://doi.org/10.1890/09-2335.1>
- Wright, S. J., Yavitt, J. B., Wurzbarger, N., Turner, B. L., Tanner, E. V. J., Sayer, E. J., ... Corre, M. D. (2011). Potassium, phosphorus, or nitrogen limit root allocation, tree growth, or litter production in a lowland tropical forest. *Ecology*, 92, 1616–1625. <https://doi.org/10.1890/10-1558.1>
- Yanoviak, S. P., Gora, E. M., Burchfield, J. M., Bitzer, P. M., & Detto, M. (2017). Quantification and identification of lightning damage in tropical forests. *Ecology and Evolution*, 7, 5111–5122. <https://doi.org/10.1002/ece3.3095>

## SUPPORTING INFORMATION

Additional supporting information may be found online in the Supporting Information section at the end of the article.

**How to cite this article:** Rutishauser E, Wright SJ, Condit R, Hubbell SP, Davies SJ, Muller-Landau HC. Testing for changes in biomass dynamics in large-scale forest datasets. *Glob Change Biol*. 2019;00:1–15. <https://doi.org/10.1111/gcb.14833>